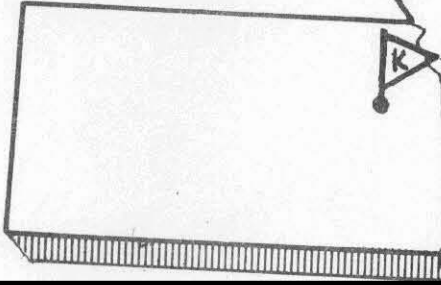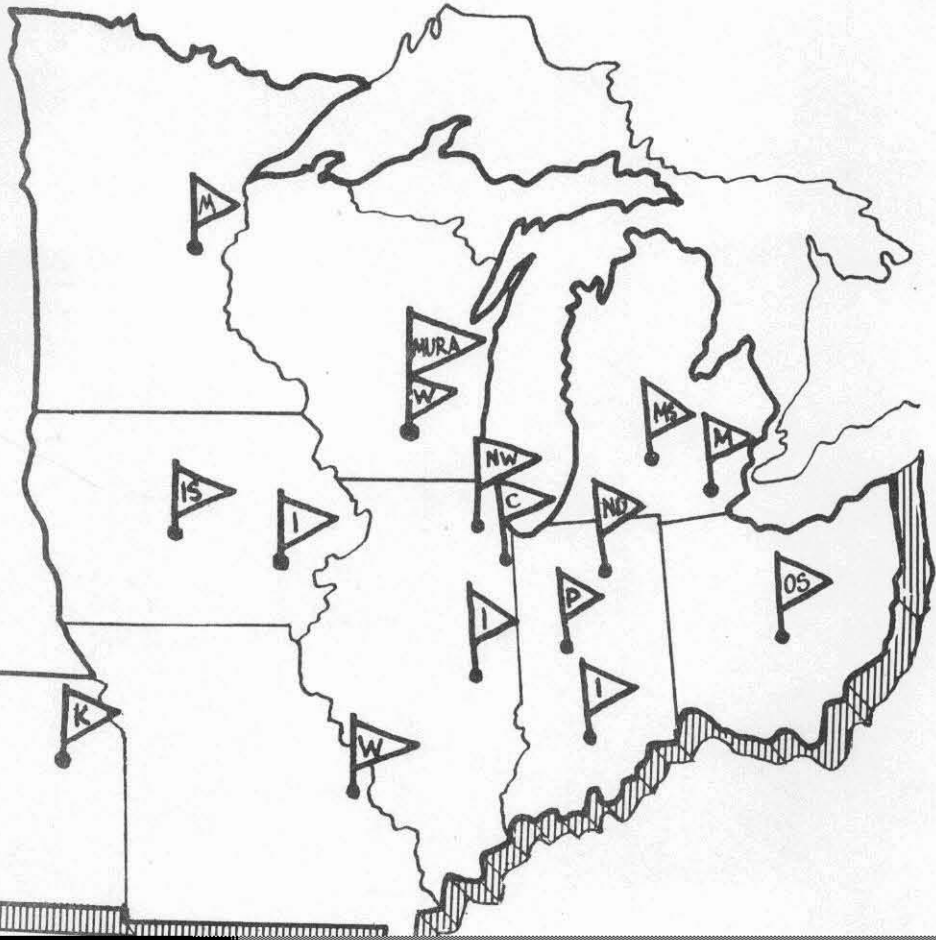# MIDWESTERN
UNIVERSITIES
RESEARCH
ASSOCIATION

DETAILED CALCULATIONS OF A SMALL MODEL

FFAG MARK Ib ACCELERATOR[*]

F. T. Cole[F] and D. W. Kerst
University of Illinois and Midwestern Universities Research
Association

A small Mark Ib ring magnet with wide radial aperture
and small momentum content has a large proportion of its
circumference in fringing fields. The calculations described
here are largely concerned with the treatment of such fringe
fields and other non-uniformities of fields or gradients on
the oscillations around the accelerator. Factors influencing
injection into such a model are also discussed.

The model has eight sectors, a final energy of about
0.5 Mev, a radius of roughly 50 cm, a radius of curvature of
about 20 cm, and a radial aperture of 15 cm. The momentum
multiplication is about 5.5 . With a minimum gap between
iron poles of about 4 cm and a straight section between
reversed field magnets of about 4 cm length, the fringing
field at the end of a magnet extends into the gap more than
2 cm. and the "straight" section is filled with fringing field.
These calculations were made to determine the influence of
such non-ideal effects on parameters which can be arrived at
simply using the matrices for sectors, straight sections and
edges assuming no fringing - "hard edged". The calculations
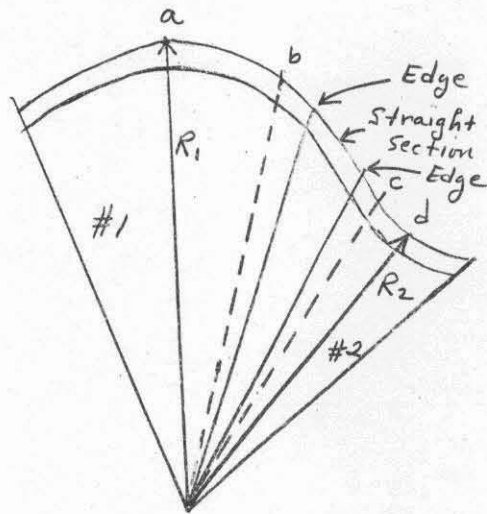using hard edges were made by Jones.

If the iron gap opened by about a factor of 5 to produce the five-fold variation of field over the radial aperture, the fringing would extend far into the magnets and orbits at the low energy radius would have a different σ from those at the high energy radius where the gap is narrow. The fringe field from the flare of the iron can be terminated by a current curtain at the ends of the magnets extending everywhere down to the minimum iron gap or the iron pole surfaces can be made essentially parallel with distributed backwindings causing the radial variation of magnetic field. The fringe field then comes from a gap of about the same size at all radii so that σ should not change with energy.

The simplest case is that for which the structure and the orbits at one radius are exactly the same as at another radius except for an enlargement or reduction factor. This factor is R/R' where R and R' are the radii of corresponding points measured from the center of the machine. σ's are geometrical quantities, so they are constant over the radial aperture and this simple "Photographic" scaling causes the gap to be smaller at small radii than at large. Thus the fringe field occupies the same proportion of the circumference at all radii. The edges of sectors lie on lines directed toward the center of the machine.

When the magnetic field changes along the path of the particle, as it does in the fringing field, the angle θ is no longer a suitable in-dependent variable because the center and radius of curvature are changing as the particle progresses. Instead the arc length s is the proper independent variable. The linear differential equations for radial and vertical oscillations about the equilibrium orbit are (x is the displacement perpendicular to the orbit):

$$\begin{cases} \dfrac{d^2 x}{ds^2} + \dfrac{1 + n(s)}{\rho^2} x = 0 \\[4mm] \dfrac{d^2 z}{ds^2} - \dfrac{n(s)}{\rho^2} z = 0 \end{cases} \tag{1}$$

ρ and n are not constants. Since $n = \dfrac{\rho}{H}\dfrac{dH}{dx}$ and $p = \dfrac{e}{c}\rho H$, we can write

$$\begin{cases} \dfrac{d^2 x}{ds^2} + \left[\left(\dfrac{eH}{cp}\right)^2 + \dfrac{c}{cp}\dfrac{dH}{dx} \right] x = 0 \\[4mm] \dfrac{d^2 z}{ds^2} - \left(\dfrac{e}{cp}\dfrac{dH}{dx} \right) z = 0 \end{cases} \tag{2}$$

where, since p is a constant along the orbit, all of the variation with s is contained in H and $\frac{dH}{dx}$, which are evaluated along the orbit.

The ratio of the fields at the centers of adjacent focussing and defocussing magnets is not determined by photographic scaling. Of the many possible cases consider two:

a) Make $H_1 = - H_2$. Then $\rho_1 = \rho_2$ and the accelerator is a Mark Ib. In this case, since $R_2 < R_1$, the spacing of orbits of different momenta is less in magnet #2 than in magnet #1. Thus $\left|\frac{dH_1}{dR_1}\right| > \left|\frac{dH_2}{dR_2}\right|$ by the factor R_1/R_2.

b) Make $\frac{dH_1}{dR_1} = - \frac{dH_2}{dR_2}$. This is achieved by making

$$\frac{H_2}{H_1} = - \frac{R_2}{R_1}$$

Case a) leaves the H^2 (centrifugal force) term of the x equation of (2) numerically the same in each magnet, while the $\frac{dH}{dx}$ term is different. Case b) keeps the gradient term the same, but requires different values for the H^2 term in different magnets. The calculations made here will be for case a).

The magnetic field is taken as constant from a to b along the arc s in the diagram of the orbit. Thus the equilibrium particle has constant radius of curvature up to b. Between b and c the magnetic field is described as $H = H_1 F (s)$. At b $F(s) = + 1$ and at c $F(s) = -1$ for

case a), so that H goes from H_1 at b to $-H_1$ at c.   From

c to d $H = H_2$ and the orbit has the same radius of curvature

as in the first magnet.

     We must first determine how H varies along the orbit;

that is, we must first find F(s).   We must also find how

$\frac{dH}{dx}$ varies along the orbit.

I. Determination of F(s)

A method for finding an approximate fringing function, F(s), will be explained.   It has a reasonable basis and sub-sequent calculations with variations on F(s) are used to test the degree to which exact knowledge of F(s) influences σ's. We know for case a) that F(s) goes from $+1$ to -1 and is zero near the center of the straight section.   The point in the magnet at which F(s) is about unity and the zero point are probably the most important features of F(s).   We notice that perpendicularly across the straight section the fields are different because of the radial gradient of field. Consider two sets of parallel pole faces with H_1 within one gap and H_2 in the other gap back from the edge.   Let the edges be parallel.   The solution to the fringing field problem is obtained by adding the solutions to the two potential problems shown below.
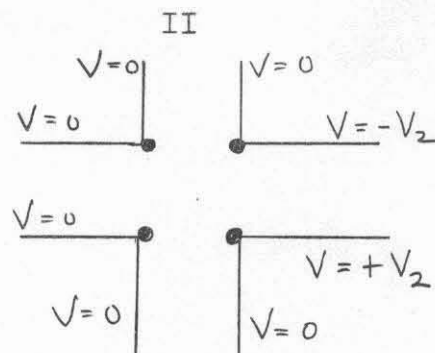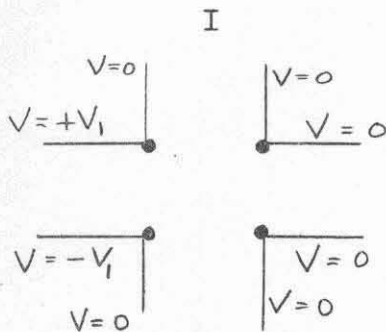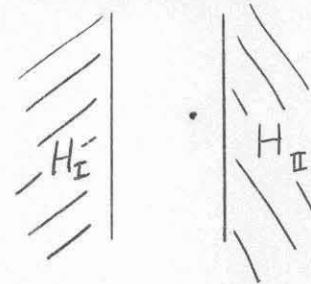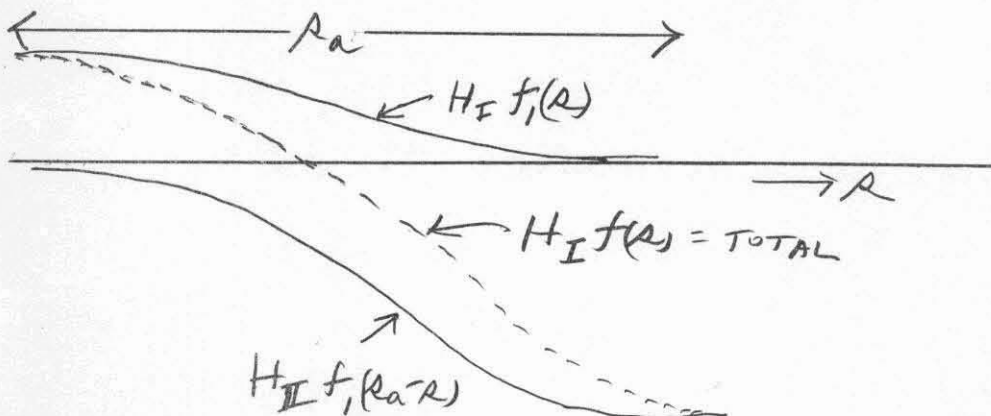
Coils are at magnet corners.

    If Δ is the position on a line perpendicular to the edges, the function $f_1 (\Delta)$ describes the magnetic field dependence in both cases if Δ is measured in the appropriate direction.
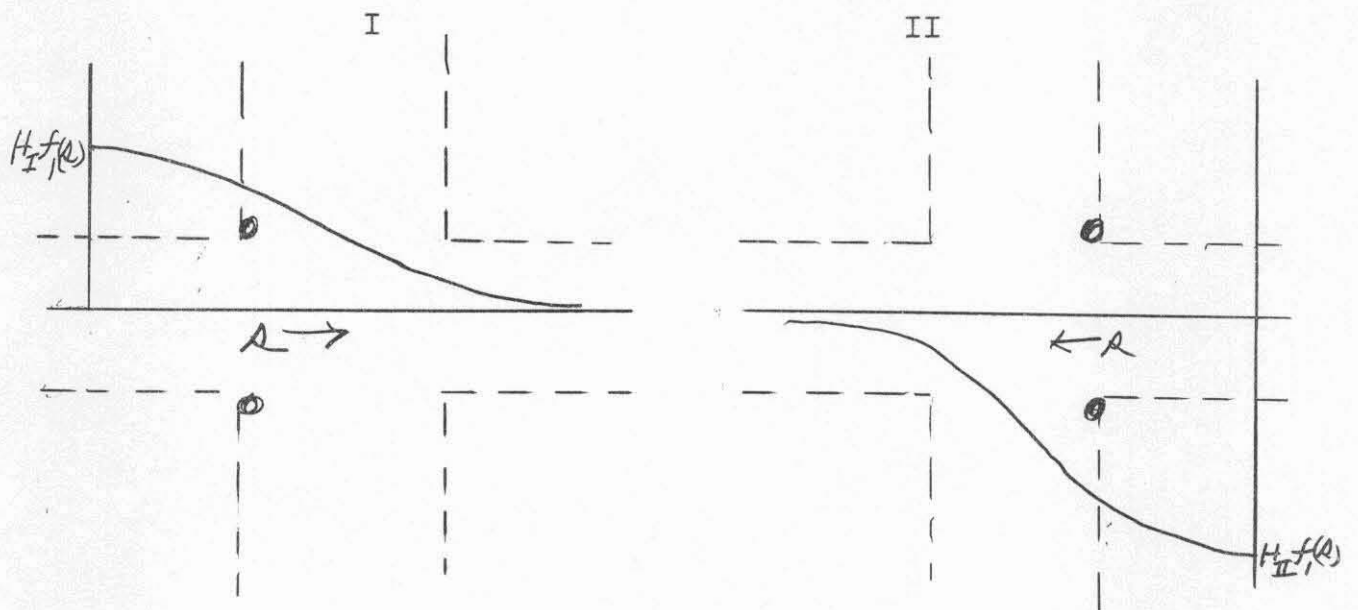
The complete solution is the sum of the two solutions:

We obtain an $f(\Delta)$ which carries all the way across the gap and into the magnets over total path of Δ_a which reaches equally far into both magnets to the point where $f_1(\Delta)$ can be taken as essentially unity.

$$f(\Delta) = f_1(\Delta) + f_1(\Delta_a - \Delta) \frac{H_{II}}{H_I} \qquad (3)$$

and

$$H(\Delta) = H_I \, f(\Delta) \qquad (4)$$

in the case of interest H_I and H_{II} are not uniform in the interior of the gaps but rather each has a gradient with a component parallel to the magnet edge and a component perpendicular to the magnet edge. We will use $f(\Delta)$ mainly to determine the position of the zero of field in the straight section by finding the ratio H_{II}/H_I for points at opposite ends of the perpendicular path across the straight section. This difference in field results from the diagonal path which a particle must follow across the straight section to go from H_1 to an equal and opposite field H_2. To find H_I and H_{II} determine the variation of field along the direction R_1 and R_2. $\quad n_1 = \frac{\rho_1}{H} \frac{dH}{dx} \quad$ is a constant along R_1 in the center of the radial focussing sector. But $\rho_1 = \rho_{10} \frac{R}{R_1} \quad$ by scaling. Also $n_2 = \frac{\rho_2}{H} \frac{dH}{dx} \quad$ is a constant along R_2 in the center of the radial defocussing sector with $\rho_2 = \rho_{20} \frac{R}{R_2}$. Integrating we have for magnet #1

$$H_1 = H_{10}\left(\frac{R}{R_1}\right)^{\frac{n_1 R_1}{\rho_{10}}} = H_{10}\left(\frac{R}{R_1}\right)^k \tag{5}$$

and in magnet #2

$$H_2 = H_{20}\left(\frac{R}{R_2}\right)^{\frac{n_2 R_2}{\rho_{20}}} = H_{20}\left(\frac{R}{R_2}\right)^k \tag{6}$$

where k is the same for both (4) and (5) for either case
a) or case b).   For case a) $\rho_{20} = \rho_{10}$ and $H_{20} = -H_{10}$

so

$$\begin{cases} H_1 = H_0\left(\frac{R}{R_1}\right)^k \\ H_2 = -H_0\left(\frac{R}{R_2}\right)^k \end{cases} \quad \text{with } k = \frac{n_1 R_1}{\rho_0} = \frac{n_2 R_2}{\rho_0} \tag{7}$$

are the field dependence equations on the center lines of
magnets. R_1 and R_2 are determined by the geometrical con-
figuration drawn for a hard edge machine, which gives a
sufficiently good orbit for
this approximate calculation.
The field at R_{E_2} is equal in
magnitude to the field at R_{E_1}
so the field at opposite ends of
$\triangle_b$ has the ratio $\left(\frac{R_{E_2} + l \sin\phi}{R_{E_2}}\right)^k$,
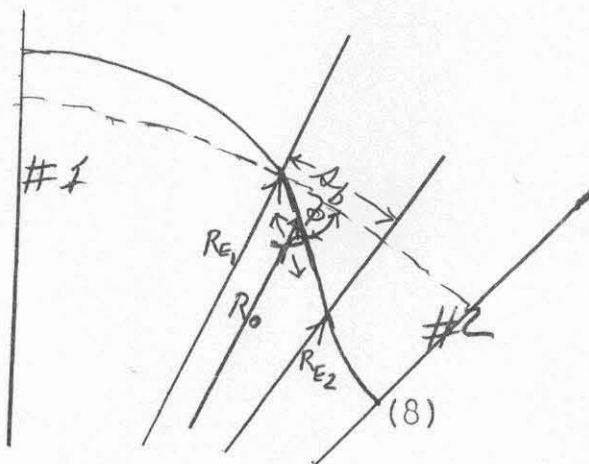
where we ignore the slight curvature of the machine

in the straight section and we use an average ϕ between the
orbit along l and the (curved) s_b.   So

$$\frac{H_{II}}{H_I} = - \left(1 + \frac{l}{R_{E_2}} \sin \overline{\phi} \right)^k$$

where R_{E_2} is taken off of
the hard edge sketch or calculated from the geometry.   One
should take a ratio slightly higher than that which has just
been calculated for hard edges because if s_b were extended
into magnet #1, lower pole strengths would be encountered;
and if it were extended into #2, higher pole strengths would
be found.   These interior increments of pole strength are
however shielded strongly by the edges.   To include this
effect we replace l by $l + \frac{G}{2}$, where G is the gap between
the magnet poles.   The zero of $f(s)$ is then at R_0.   By (3)

$$f_1(s_0) = f_1(s_a - s_0)\left[1 + \frac{(l + \frac{G}{2})\sin\overline{\phi}}{R_{E_2}} \right]^k \quad (8)$$

An F(s) which describes the field variation along the
orbit can then be constructed approximately by forming a
symmetrical

$$f(s) = f_1(s) - f_1(s_a - s) \quad (9)$$

which carries one between equal and opposite fields.   If s is
replaced by s cos $\overline{\phi}$ we have an approximate function along the
path of the particle.   But this function must have its s

distorted so that its zero occurs on the radial line R_o containing s_o. This can be done graphically or by replacing s by $\left(S + \Delta \sin \dfrac{\pi s}{s_a} \right) \cos \bar{\phi}$, which displaces the zero by an amount Δ. The final function is approximated by a power series for use in the differential equation(2).

$f_1(s)$ was calculated by Vogt-Nilsen and graphs for various ratios of pole separation to gap are given in Graph 1.

GRAPH 1

V = MAGNETIC POTENTIAL

$\bar{B} = -\nabla V$

$B_0 = -2 V_0 / G$
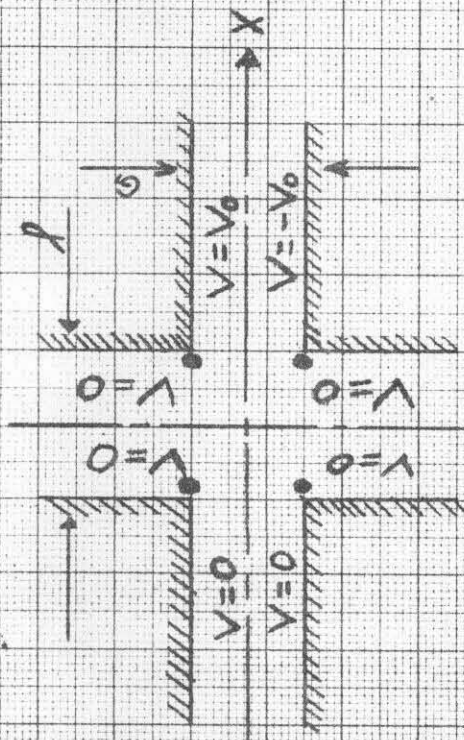
FOR $\ell/G = \infty$

$$X/G = -\kappa_T \left[(B/B_0)^{-3/2} + \frac{1}{2} \ln \frac{1-(B/B_0)^{3/2}}{1+(B/B_0)^{3/2}} \right]$$

FOR $\ell/G = 0$

$$B/B_0 = (1 + e^{-2\pi X/G})^{-1}$$

V = MAGNETIC POTENTIAL

$\bar{B} = -\nabla V$

$B_0 = -2V_0/G$

→ X

B/B_0

1.0

.8

.6

.4

.2

$y/G = 0$

$y/G = 0.5$

$y/G = 1$

$y/G = \infty$

→ X/G

0   0.5

-0.5

-1.0

-1.5

V = 0

V = 0

V = 0

V = V₀

V = -V₀

V = -V₀

V = V₀

ℓ

G

FOR $y/G = \infty$

$$X/G = -\frac{1}{\pi}\left[\left(\frac{B}{B_0}\right)^{-3/2} + \frac{1}{2}\,Ln\,\frac{1-\left(\frac{B}{B_0}\right)^{3/2}}{1+\left(\frac{B}{B_0}\right)^{3/2}}\right]$$

FOR $X/G = 0$

$$\frac{B}{B_0} = Tanh\,\pi\,X/G$$
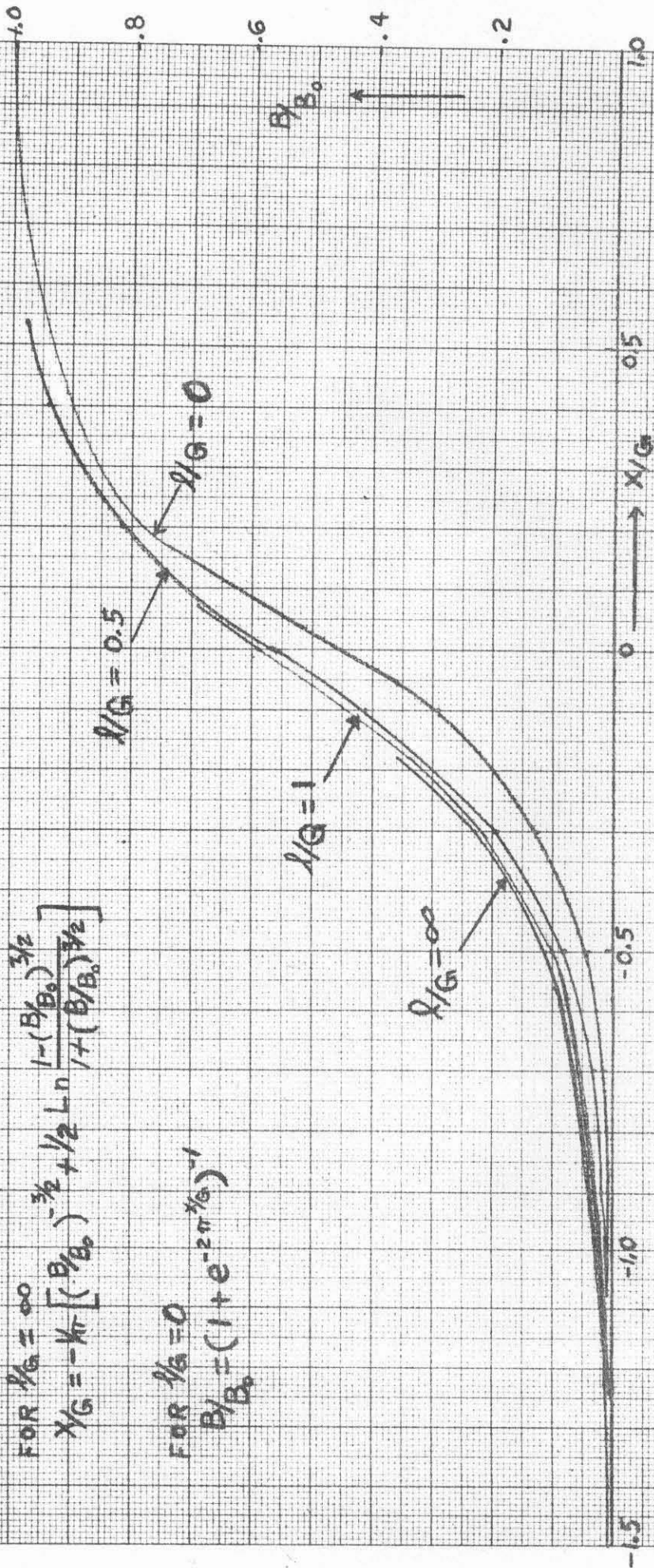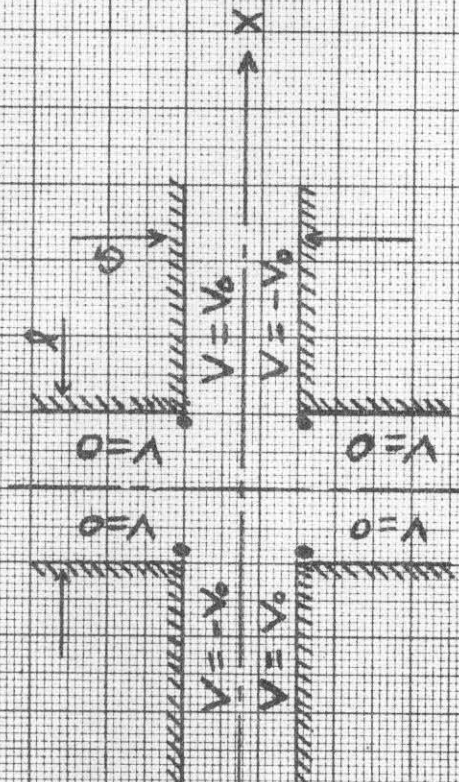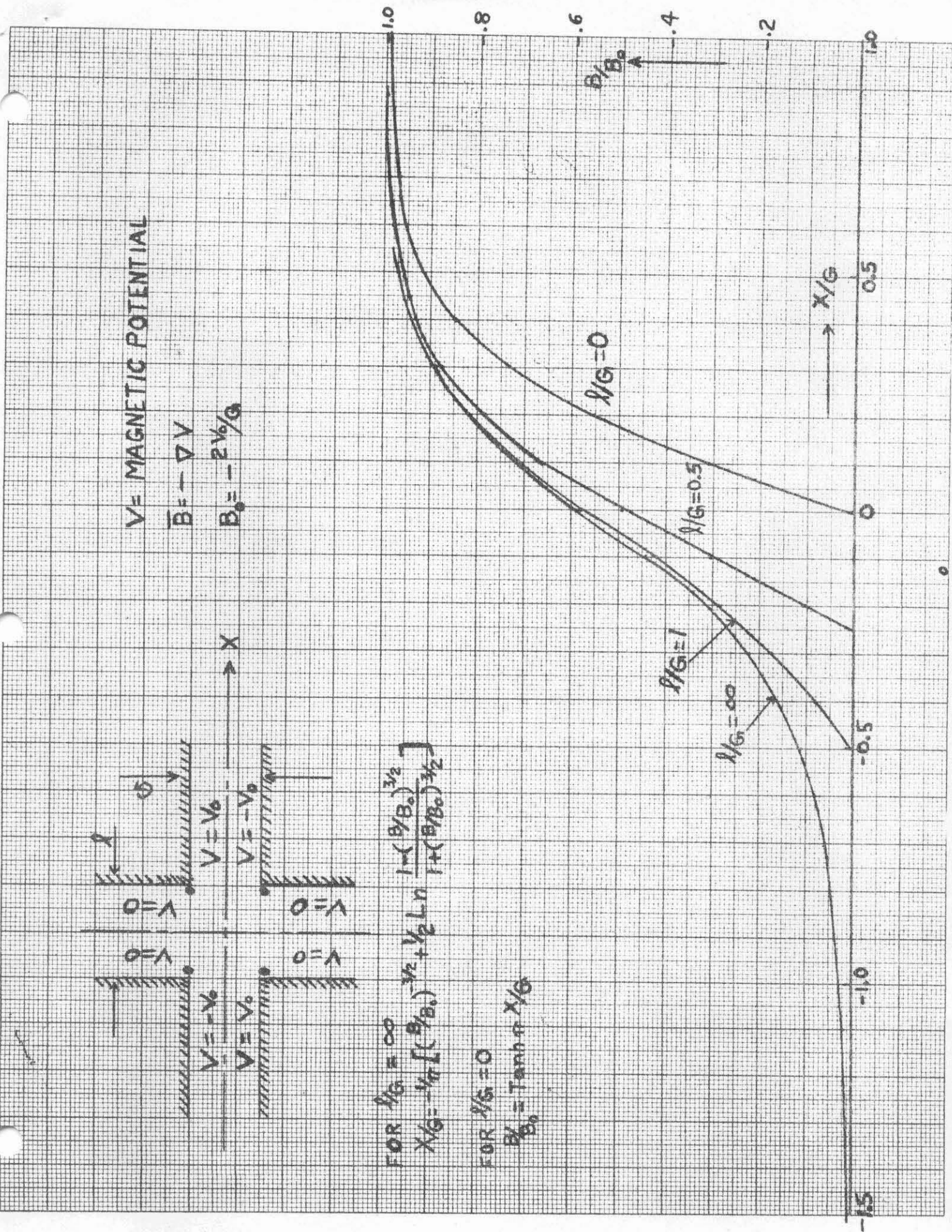
II. Variation of $\dfrac{dH}{dx}$ Along the Orbit

$\dfrac{dH}{dx}$ varies in the regions where $|F(s)| = 1$ because
of the variation of perpendicular separation of adjacent
scaled orbits representing slightly different momenta.

$$\Delta x = \Delta R \cos \phi$$

and

$$\Delta R = \Delta R_1 \frac{R}{R_1}$$

Then

$$\frac{dH}{dx} = \frac{dH_1}{dx_1} \frac{R_1}{R(s)} \sec \phi(s) \qquad (10)$$
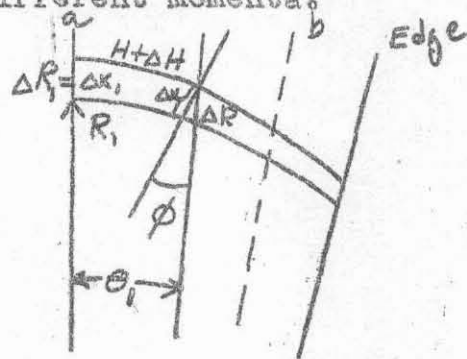
This variation of $\dfrac{dH}{dz}$ occurs
everywhere. In addition, when $\dfrac{dF}{ds} \neq 0$, particles of
different amplitudes see different fields because the edges
are not perpendicular to the orbits. Thus in (2) we must
use

$$\frac{dH}{dx} = \frac{dH_1}{dx_1} \frac{R_1}{R(s)} \sec \phi(s) + H_1 \frac{dF}{ds} \frac{\delta s}{\delta x}$$

$$(11)$$

where the first term comes from (10) and in the second term,
δs is the change in path length when a particle is moved
a distance δx perpendicular to the orbit.
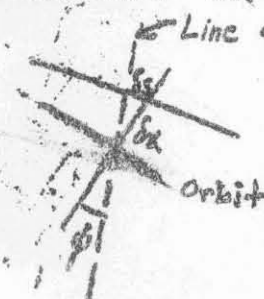
From the figure, $\dfrac{\delta s}{\delta x} \cong \tan \phi$

and the differential equations (2) become

$$\begin{cases} \dfrac{d^2 x}{ds^2} + \left\{ \dfrac{F^2(s)}{\rho_0{}^2} + \dfrac{n_1}{\rho_0{}^2} F(s) \dfrac{R_1}{R(s)} \sec\phi(s) + \dfrac{F'(s)\tan\phi(s)}{\rho_0} \right\} x = 0 \\[4mm] \dfrac{d^2 \mathfrak{z}}{ds^2} - \left\{ \dfrac{n_1}{\rho_0{}^2} F(s) \dfrac{R_1}{R(s)} \sec\phi(s) + \dfrac{F'(s)\tan\phi(s)}{\rho_0} \right\} \mathfrak{z} = 0 \end{cases} \qquad (12)$$

where

$$\rho_0 = \frac{cp}{eH_1}$$

III. Hard Edge Orbits

When we neglect the fringing fields altogether, b
and c coincide with the edges of magnets 1 and 2 and $F(s) = 0$
between them.   Then $F'(s)$ is zero except at the edges, where
it is $\frac{1}{I}\delta(s - s_0)$ where $\delta(s)$ is the Dirac δ -function.
Then there is an infinite acceleration and a discontinuous
change in velocity by an amount $\frac{\tan\phi}{\rho_0} x$ at each edge.   The
transformation matrix for edges clearly has the form

$$\begin{pmatrix} 1 & 0 \\ \dfrac{\tan\phi}{\rho_0} & 1 \end{pmatrix} \tag{13}$$

and the matrix for the straight section is multiplied on the
right and left by matrices of this form with appropriate
ϕ 's.

$$\delta = \frac{l}{\rho}$$

$$\beta_1 - \beta_2 = \frac{\pi}{N}$$

$$\tan\epsilon = \frac{\delta}{2} \tag{14}$$
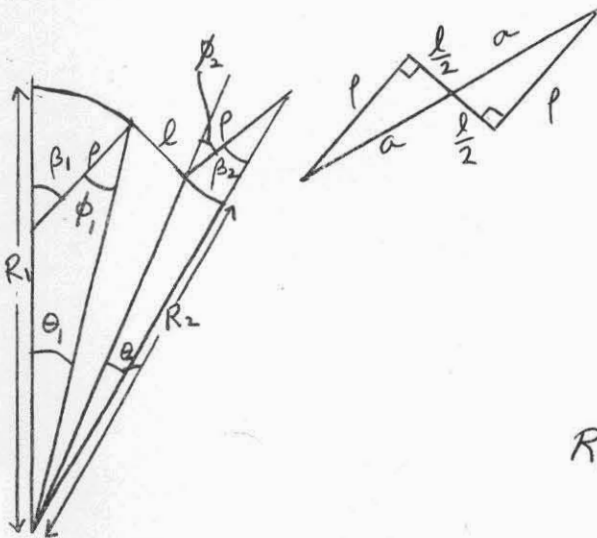
$$a = \sqrt{1 + \left(\frac{\delta}{2}\right)^2}$$

$$R_1 - \rho = 2a\,\frac{\sin(\beta_2 + \epsilon)}{\sin\frac{\pi}{N}}$$

$$R_2 + \rho = 2a\,\frac{\sin(\beta_1 + \epsilon)}{\sin\frac{\pi}{N}}$$

$$\tan \theta_1 = \frac{\rho \sin \beta_1}{R_1 - \rho + \rho \cos \beta_1}$$

$$\tan \theta_2 = \frac{\rho \sin \beta_2}{R_2 + \rho - \rho \cos \beta_2}$$

$$\phi_1 = \beta_1 - \theta_1 \quad ; \quad \phi_2 = \beta_2 + \theta_2$$

These geometric formulae show that photographic scaling is possible, since all distances are given in terms of ρ .

We have calculated σ_x and σ_z as functions of n and β_1 . In these calculations we have partly included the effect of equation(10) by taking n in the reversed field magnet as $n_2 = n_1 \frac{R_1}{R_2}$. For the radial motion, calling

$$\left\{ \begin{array}{l} \omega_1 = \sqrt{1 + n_1} \\[4pt] c_1 = \cos \omega_1 \beta_1 \\[4pt] s_1 = \sin \omega_1 \beta_1 \\[4pt] \omega_2 = \sqrt{n_2 - 1} \\[4pt] c_2 = \cosh \omega_2 \beta_2 \\[4pt] s_2 = \sinh \omega_2 \beta_2 \\[4pt] \xi_1 = 1 + \delta \tan \phi_1 \\[4pt] \xi_2 = 1 + \delta \tan \phi_2 \\[4pt] \eta = (\tan \phi_1 + \tan \phi_2) + \delta \tan \phi_1 \tan \phi_2 \end{array} \right. \tag{15}$$

then the transformation matrix from the center of magnet #1
to the center of magnet #2 has the form

$$\begin{pmatrix} a & b \\ c & d \end{pmatrix} \tag{16}$$

where

$$
\left\{
\begin{aligned}
a &= \xi_1 c_1 c_2 - \delta\omega_1 s_1 c_2 + \frac{\eta}{\omega_2} c_1 s_2 - \frac{\xi_2 \omega_1}{\omega_2} s_1 s_2 \\
b &= \delta c_1 c_2 + \frac{\xi_1}{\omega_1} s_1 c_2 + \frac{\xi_2}{\omega_2} c_1 s_2 + \frac{\eta}{\omega_1 \omega_2} s_1 s_2 \\
c &= \eta c_1 c_2 - \xi_2 \omega_1 s_1 c_2 + \xi_1 \omega_2 c_1 s_2 - \delta\omega_1\omega_2 s_1 s_2 \\
d &= \xi_2 c_1 c_2 + \frac{\eta}{\omega_2} s_1 c_2 + \delta\omega_2 c_1 s_2 + \xi_1 \frac{\omega_2}{\omega_1} s_1 s_2
\end{aligned}
\right. \tag{17}
$$

Since the center of each magnet is a point of symmetry
of the differential equation, the matrix to transform through
the rest of the sector is just the time-reversed matrix

$$\begin{pmatrix} d & b \\ c & a \end{pmatrix} \tag{18}$$

and

$$\cos \sigma = ad + bc = 2ad - 1$$

For the z-motion, 1 and 2 are interchanged, $\omega_1 = \sqrt{n_1}$, $\omega_2 = \sqrt{n_2}$, and ϕ_1 and ϕ_2 became the negatives of their previous values.

The results are shown in graphs 2 and 3. The importance of the edge focussing is evident in the curves. The vertical motion is quite insensitive to n for a given β. A calculation of σ_3 without edge effects shows that the vertical motion is unstable ($\cos \sigma_3 > 1$). The radial motion is less strongly affected. Without edges, in most cases the radial motion is stable, but close to the limit ($\sigma_x \sim \pi$).

On the curves integral, half-integral and quarter - integral wavelengths are shown.

It is difficult to make a general statement about the effect of the n-variations in all machines. Since n is larger at the ends of magnets than at the centers, one can say quali- tatively that there is an added lens at each edge due to this effect; this lens is focussing in focussing sectors and defo- cussing in defocussing sectors, but the focal length of the lens pair depends, of course, on the length of the straight section. We have treated this effect in an ad-hoc way; we approximate the curve of $n(S)$ by several steps. In the one case treated, we find

COS σ_x AND COS σ_x AS FUNCTIONS OF β_1
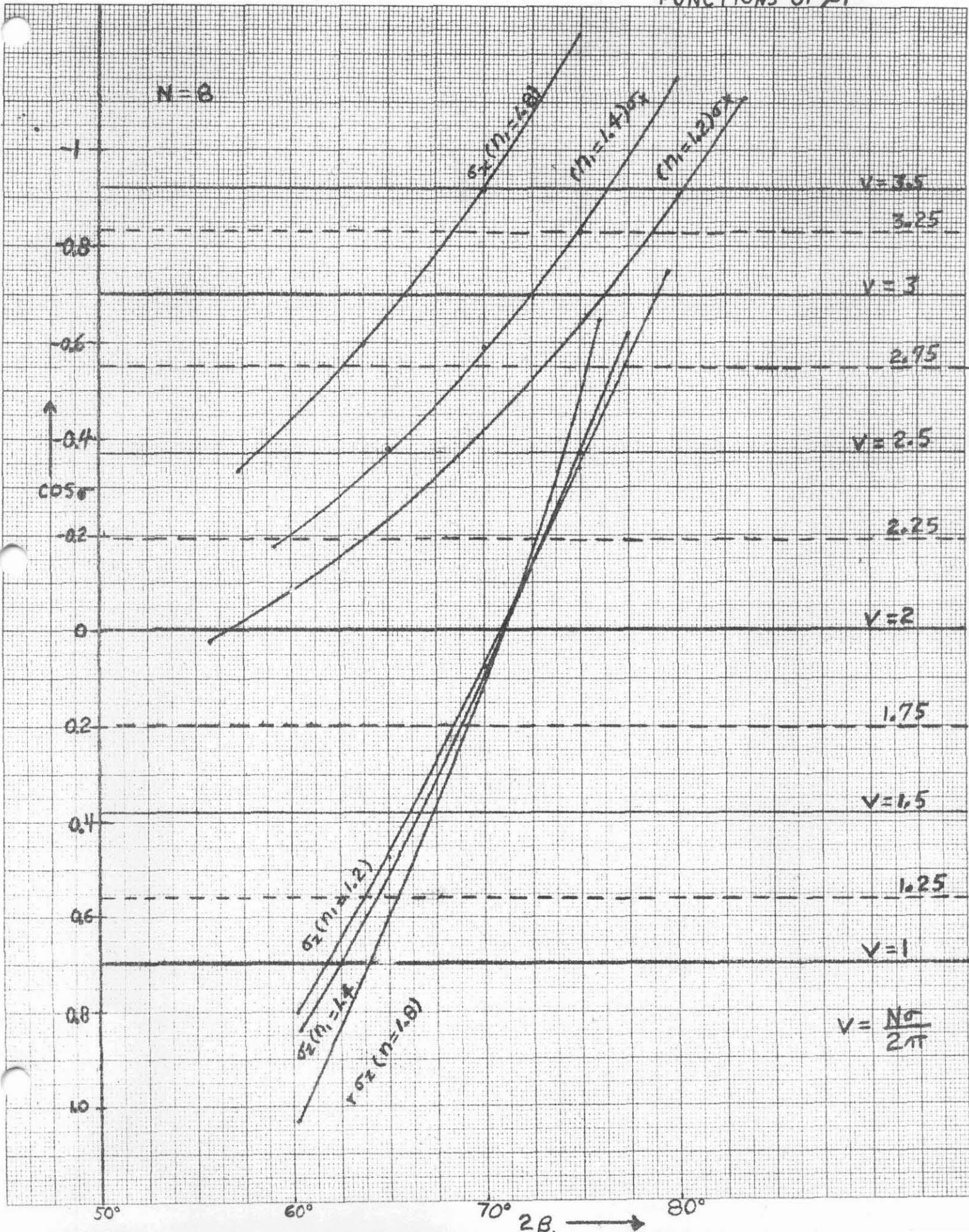
$\cos\sigma_x$ AND $\cos\sigma_z$ AS FUNCTIONS OF n_{10}
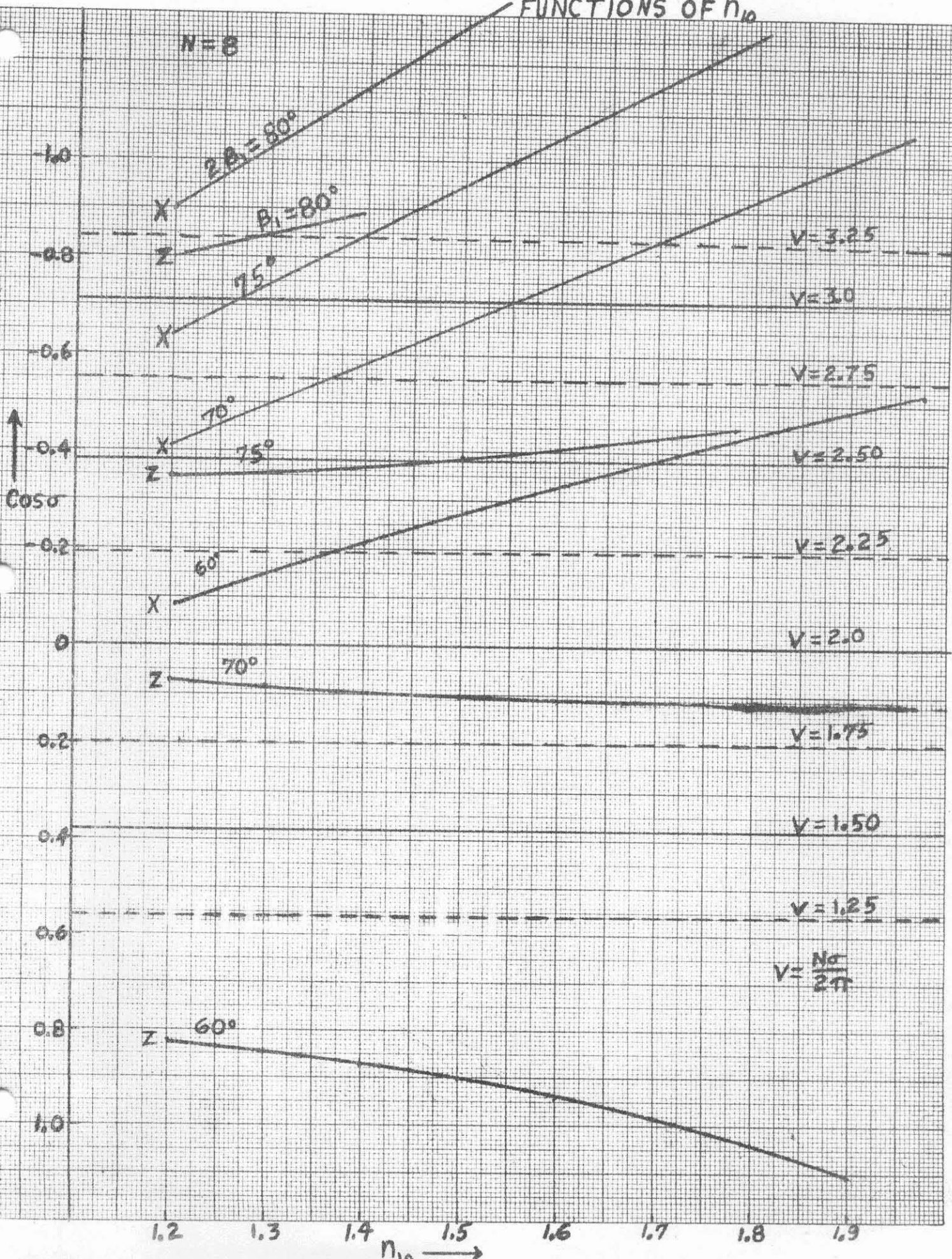
	Without n-variation	With n-variation
ν_x	2.87	2.94
ν_z	1.74	1.68

Because of the greater length of the radial focussing sector, the equivalent lenses at its edges are stronger. Thus ν_x increases and ν_z decreases.

IV. Soft Edge Orbits

We are interested mainly in the effects of fringing fields on the frequencies of betatron oscillations. However, we must treat the problem of equilibrium orbits in soft edge fields because the oscillations depend on the position of the equilibrium orbits.

One may ask two distinct questions about equilibrium orbits in soft edge fields:

1. Can one construct equilibrium orbits in soft-edge fields without reference to hard edge orbits; can the geometry above be carried through for soft edges?

2. If the edges are "softened" in a fixed geometry, how do the orbits move?

The second question is closely related to the question of "tuning" the oscillations to a desired frequency in a fixed geometry, i.e., in an accelerator already constructed. The "tuning" and the second question will be discussed in a later report.

To discuss the first question, let us describe the equilibrium orbit by the variables ϕ , the angle which the perpendicular to the orbit makes with lines radial from the center of the machine and R, the distance of the orbit from the center of the machine. ϕ changes because of the bending due to the magnetic field and because of the rotation of the radial line. The bending due to the magnetic field is, in distance ds

$$d\psi = \frac{d\phi}{p} = \frac{\frac{e}{c}\frac{ds}{dt}\cdot dt \cdot H_0 \, F(s)}{\frac{e}{c}\rho_0 H_0}$$

$$= \frac{F(s)\, ds}{\rho_0}$$

so that
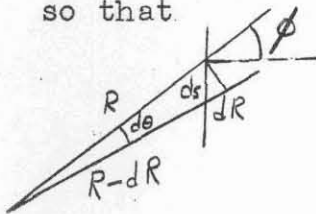
$$\frac{d\phi}{ds} = \frac{1}{\rho_0} F(s) - \frac{d\theta}{ds} \qquad\qquad (19)$$

$$= \frac{1}{\rho_0} F(s) - \frac{\cos\phi}{R} \qquad\qquad (19a)$$

and

$$\frac{dR}{ds} = - \sin\phi \qquad\qquad (20)$$

The meaning of the ϕ equation is not quite unambiguous, because we do not know F(s) exactly along the orbit until we have solved the equation to find the orbit.   But we can use the equation to find what features of the motion depend on F(s).

The equilibrium orbit has the period of the sector and is

symmetric about the centers of the magnets.

Thus

$$\phi = 0$$

$$at \quad \theta = 0 \quad and \quad \theta = \frac{\pi}{N} \tag{21}$$

Between a and b, $F(s) = 1$ and between c and d, $F(s) = -1$

By integrating (19) from a to b,

$$\phi_1' = \frac{S_1'}{\rho_0} - \theta_1' = \beta_1' - \theta_1' \tag{22}$$

and from c to d,

$$\phi_2' = \beta_2' + \theta_2' \tag{23}$$

In the magnets we have the geometrical equations
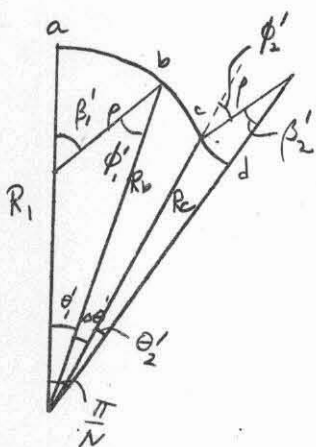
$$\begin{cases} R_b = \rho_0 \dfrac{\sin \beta_1'}{\sin \theta_1'} \\[2mm] R_1 - \rho_0 = \rho_0 \dfrac{\sin \phi_1'}{\sin \theta_1'} \\[2mm] R_2 + \rho_0 = \rho_0 \dfrac{\sin \phi_2'}{\sin \theta_2'} \\[2mm] R_c = \rho_0 \dfrac{\sin \beta_2'}{\sin \theta_2'} \end{cases} \tag{24}$$

We connect these across the straight section by using
(19) and (20).   We call $\Delta \theta'$ the angle between R_b and R_c
($\theta_1' + \theta_2' + \Delta \theta' = \dfrac{\pi}{N}$), S the length of the orbit between

b and c and

$$I = \frac{\int_b^c F(s)\, ds}{S}$$

(25)

I is, of course, dimensionless.

By integrating (19) from b to c,

$$\phi_2' = \phi_1' + \frac{S'I}{\rho_0} - \Delta\theta'$$

and, with (22) and (23),

$$\beta_2' + \theta_2' = \beta_1' - \theta_1' + \frac{S'I}{\rho_0} - \Delta\theta'$$

or

$$\beta_1' - \beta_2' + \frac{S'I}{\rho_0} = \frac{\pi}{N}$$

(26)

From (19) and (19a)

$$\Delta\theta = \frac{\cos\phi_b}{R_b} S' + \alpha$$

(27)

and from (22)

$$R_c = R_b - S\sin\phi_b + \delta$$

(28)

where α and δ are correction terms. We estimate the values of α and δ by using the values of ϕ_b, R_b and S from the hard-edge orbit. There is a cancellation between the two largest terms which makes δ very small and some cancellation in α. That is

$$\delta \cong - \cos\phi_b \phi_b' \frac{S'^2}{2} - \left(-\sin\phi_b \phi_b'^2 + \cos\phi_b \phi_b'' \right) \frac{S'^3}{6} - \ldots$$

$$\cong - \cos\phi_b \left[\frac{1}{\rho_0} - \frac{\cos\phi_b}{R_b} \right] \frac{S'^2}{2} +$$

$$+ \sin\phi_b \left(\frac{1}{\rho_0} - \frac{\cos\phi_b}{R_b} \right)^2 \frac{S^3}{6} - \cos\phi_b \left[-\frac{2}{\rho S'} + \frac{\sin\phi_b \phi_b'}{R_b} - \frac{\sin\phi_b \cos\phi_b}{R_b^2} \right] \frac{S'^3}{6}$$

$$\cong \cos\phi_b \left[\frac{\cos\phi_b}{2R_b} - \frac{1}{6\rho_0} \right] S'^2 + \text{smaller terms}$$

and the coefficient of S^2 almost vanishes for any R_b and
ϕ_b in the range encountered. Proceeding in the same way,
we estimate $\alpha \cong 0.004$, which we use. Equations
(24), (26), (27), and (28) are thus seven equations in the
variables R_1, R_2, R_b, R_c, β_1', β_2', S, I, ρ_0, θ_1', θ_2'.
We choose I, ρ_0, θ_1' and θ_2' and calculate the remaining
seven. Because of the smallness of α and δ , the equations
do not depend on the shape of $F(s)$ but only on I, the net
turning through the fringe field. Thus many different field
shapes which have the same value of I have very nearly the
same equilibrium orbit.

We choose ρ_0 = 20 cm to fix the size of the machine.
Of course all distances scale, so that we are really consider-
ing one member of a one-parameter family of orbits. θ_1' and
θ_2' may be chosen arbitrarily, but we are guided by the
fringe-field calculations of Vogt-Nilsen and choose them corres-
ponding to desirable θ_1 and θ_2. The only approximation in our
procedure is in the choice of I, due to our lack of knowledge

of the exact functional form of F(s). We calculate I along the
hard-edge orbit. The value of I depends most critically on the
shift of the zero of F(s), since most of the contribution to
the integral from the region where $F(s) < 0$ is cancelled by
contributions from the region where $F(s) > 0$.

We eliminate between the equations above to get

$$\cos\left(\frac{I(\Delta\theta' - \alpha)}{\sin\theta_1'[\cot\beta_1'\cos\theta_1' + \sin\theta_1']} - \frac{\pi}{8}\right) + \cot\beta_1'\sin\left(\frac{I(\Delta\theta' - \alpha)}{\sin\theta_1'[\cot\beta_1'\cos\theta_1' + \sin\theta_1']} - \frac{\pi}{8}\right)$$

$$= \frac{\sin\theta_2'}{\sin\theta_1'}\left\{1 + \frac{\delta}{R_b} - (\Delta\theta - \alpha)\frac{\cos\theta_1' - \sin\theta_1'\cot\beta_1'}{\cot\beta_1'\cos\theta_1' + \sin\theta_1'}\right\} \quad (29)$$

where β_1' is the only unknown $(\Delta\theta' = \frac{\pi}{8} - \theta_1' - \theta_2')$ (29) is
solved by trial. Mr. T. B. Elfe has aided us in the deriva-
tion of (31) and has done the numerical solutions.

With a little practice it is possible to guess a trial β_1'
quite accurately, so that the solution takes only a few trials.

There are two checks on the correctness of the solution.
R_c may be calculated from either the last of (26) or from (30).
Also, ϕ and R may be expanded in power series about b and c
and their values at the point where $F(s) = 0$ may thus be calcu-
lated in two ways. We find that the calculations are not sensi-
tive to the values of δ and α used.

Several orbits are given below

	θ_1'	θ_2'	I	β_1'	β_2'	$R_1^{(cm)}$	$R_b^{(cm)}$
1.	10.55°	2.26°	-0.0116	0.4951	0.0972	53.42	51.90
2.	11.32	3.03	-.0145	.5276	.1295	53.02	51.30
3.	10.55	2.26	0	.4887	.0960	52.76	51.28
4.	9.975	2.83	-.0116	.5355	.1368	60.79	58.89
5.	10.26	2.54	-.0116	.5138	.1155	56.89	55.19

	$R_c^{(cm)}$	$R_2^{(cm)}$	$S'^{(cm)}$	ϕ_1'	ϕ_2'	ϕ_0	$R_0^{(cm)}$
1.	49.16	49.12	9.0011	0.3110	0.1367	0.3403	50.38
2.	48.86	48.63	7.494	.3301	.1824	.3432	49.99
3.	48.61	48.48	8.876	.3046	.1354	.3328	49.80
4.	55.24	55.01	10.399	.3613	.1862	.4074	56.90
5.	52.02	51.84	9.653	.3347	.1599	.3725	53.42

where ϕ_0 and R_0 are the values where $F(s) = 0$.

Case 1 is the orbit in a fringe field from a gap scaled up "photographically" from 4 cm at the injection radius to 5.644 cm at the outer radius, in order to keep σ constant across the aperture. The geometry is that which gives, in the hard edge approximation, $\nu_x = 2.87$ and $\nu_3 = 1.74$.

Case 2 is the orbit in a 4 cm gap, i.e., one where the gap is not scaled up.

Case 3 is the orbit in the same geometry, but with the shift of the zero of $F(s)$ neglected.

Cases 4 and 5 are "scaled-up" gaps, used to search for desired $\sqrt{s'}$.

V. Oscillations about soft-edge orbits

The oscillations satisfy the differential equations

$$\begin{cases} \dfrac{d^2 x}{ds^2} + \left[\dfrac{1}{\rho_0^2} F^2(s) + \dfrac{m_1}{\rho_0^2} F(s) \dfrac{R_1}{R(s)} \sec\phi(s) + \dfrac{dF}{ds} \dfrac{\tan\phi(s)}{\rho_0} \right] x = 0 \\[4mm] \dfrac{d^2 z}{ds^2} - \left[\dfrac{m_1}{\rho_0^2} F(s) \dfrac{R_1}{R(s)} \sec\phi(s) + \dfrac{dF}{ds} \dfrac{\tan\phi(s)}{\rho_0} \right] z = 0 \end{cases} \tag{30}$$

We first expand $\dfrac{R_1}{R(s)} \sec\phi(s)$ using equations (19a) and (20). We define

$$\begin{cases} \phi_0 = \phi(0) \\ s_0 = \sec\phi_0 \\ s_0' = \sec\phi_0 \tan\phi_0 \\ s_0'' = \sec\phi_0 (1 + 2\tan^2\phi_0) \\ s_0^{(n)} = \dfrac{d^n}{d\phi^n}(\sec\phi)\Big|_{s=0} \end{cases} \tag{31}$$

and thus

$$\frac{R_1}{R(s)} \sec\phi(s) = \frac{R_1}{R_0}\left\{ s_0 + \left(s_0' \phi_0' + \frac{\sin\phi_0}{R_0} \right) s + \right.$$
$$\left. + \left[\tfrac{1}{2}(s_0'' \phi_0'^2 + s_0' \phi_0'') + \frac{\sin^2\phi_0}{R_0} + \frac{1}{2R_0}(\cos\phi_0)\phi_0' \right] s^2 + \ldots \right\}$$

$$= \frac{R_1}{R_0}\left\{ s_0 + s_1 s + s_2 s^2 + \ldots \right\} \tag{32}$$

where ϕ_0', ϕ_0'', etc. may be calculated from (19a) and (20).

In the same way we expand $\tan\phi$, calling

$$
\begin{cases}
t_0 = \tan \phi_0 \\
t_0' = \sec^2 \phi_0 \\
t_0'' = 2 \sec^2 \phi_0 \tan \phi_0 \\
t_0^{(n)} = \dfrac{d^n}{d\phi^n}(\tan \phi)\Big/_{s=0}
\end{cases}
\tag{33}
$$

so that

$$
\tan \phi_{(s)} = t_0 + t_0' \phi_0' s + \tfrac{1}{2}(t_0'' \phi_0'^2 + t_0' \phi_0'')s^2 + \dots \tag{34}
$$

$$
= t_0 + t_1 s + t_2 s^2 + \dots
$$

In the region where $|F(s)| \neq 1$, we will approximate it by a power series. We expand about the point where $F(s) = 0$ and use odd powers of s, with different series for $s < 0$ and $s > 0$, since $F(s)$ is not an odd function. Thus we assure a form

$$
F(s) = a_1 s + a_3 s^3 + a_5 s^5 + \dots \tag{35}
$$

Call

$$
\begin{cases}
\dfrac{n_1 R_1}{\rho_0^2 R_0} s_n = A_n \\
\dfrac{t_n}{\rho_0} = B_n \\
\dfrac{1}{\rho_0^2} = C
\end{cases}
\tag{36}
$$

Then the differential equation (29) is

$$
\frac{d^2 x}{ds^2} + \left\{ C F^2(s) + (A_0 + A_1 s + A_2 s^2 + \dots)F(s) + F'(s)(B_0 + B_1 s + B_2 s^2 + \dots) \right\} x = 0
$$

or

$$
\frac{d^2 x}{ds^2} + \left\{ C[a_1^2 s^2 + 2a_1 a_3 s^4 + a_3^2 s^6 + 2a_1 a_5 s^6 + \dots] + (A_0 + A_1 s + A_2 s^2 + \dots)(a_1 s + a_3 s^3 + \dots) + (B_0 + B_1 s + B_2 s^2 + \dots)(a_1 + 3a_3 s^2 + 5a_5 s^5 + \dots) \right\} x = 0
$$

We introduce the abbreviations

$$
\begin{cases}
a_1^2 C = \gamma_1 \\
2 a_1 a_3 C = \gamma_2 \\
a_3^2 C = \gamma_3 \\
a_n A_m = \alpha_{nm} \\
n\, a_n B_m = \beta_{nm}
\end{cases}
\qquad
\begin{array}{l}
\text{and} \\[4pt]
\displaystyle\sum_{m+n=p} \beta_{mn} = S_p
\end{array}
\tag{37}
$$

A solution is assumed of the form

$$
x = \sum_n b_n s^n
\tag{38}
$$

and, by substituting,

$$
\begin{cases}
b_2 = -\tfrac{1}{2} S_1\, b_0 \\[6pt]
b_3 = -\tfrac{1}{6}\big[(\alpha_{10} + S_2) b_0 + S_1 b_1 \big] \\[6pt]
b_4 = -\tfrac{1}{12}\Big[\big(\gamma_1 + \alpha_{11} + S_3 - \tfrac{1}{2} S_1^2\big) b_0 + (\alpha_{10} + S_2) b_1 \Big] \\[6pt]
b_5 = -\tfrac{1}{20}\Big\{ \big[\alpha_{30} + \alpha_{12} + S_4 - \tfrac{2}{3} S_1(\alpha_{10} + S_2)\big] b_0 + \\
\qquad\qquad + \big[\gamma_1 + \alpha_{11} + S_3 - \tfrac{1}{6} S_1^2\big] b_1 \Big\} \\[6pt]
b_6 = -\tfrac{1}{30}\Big\{ \big[\gamma_2 + \alpha_{31} + \alpha_{13} + S_5 - \tfrac{7}{12} S_1(\gamma_1 + \alpha_{11} + S_3) - \\
\qquad\qquad - \tfrac{1}{6}(\alpha_{10} + S_2)^2 + \tfrac{1}{24} S_1^3 \big] b_0 + \\
\qquad\qquad + \big[\alpha_{30} + \alpha_{12} + S_4 - \tfrac{1}{4} S_1(\alpha_{10} + S_2)\big] b_1 \Big\}
\end{cases}
\tag{39}
$$

etc.

Now $X(0) = b_0$ and $X'(0) = b_1$, so that the two solutions with $b_1 = 0$ or $b_0 = 0$ are linearly independent. The solution with $b_0 = 0$ satisfies $x(0) = 0$. Since these are the conditions satisfied by the elements M_{1j} of the transformation matrix, these solutions are directly these elements. Their derivatives are the elements M_{2j}. Thus we can calculate the transformation matrix through any part of the fringe field, using

$$M_{11} = 1 - \frac{1}{2} J_1 s^2 - \frac{1}{6}(\alpha_{10} + J_2) s^3 - \frac{1}{12}(\gamma_1 + \alpha_{11} + J_3 - \frac{1}{2} J_1^2) s^4$$

$$- \frac{1}{20}[\alpha_{30} + \alpha_{12} + J_4 - \frac{2}{3} J_1 (\alpha_{10} + J_2)] s^5 -$$

$$- \frac{1}{30}[\gamma_2 + \alpha_{13} + \alpha_{31} + J_5 - \frac{7}{12} J_1(\gamma_1 + \alpha_{11} + J_3) - \frac{1}{6}(\alpha_{10} + J_2)^2 + \frac{1}{24} J_1^3] s^6 + \ldots$$

$$M_{21} = - J_1 s - \frac{1}{2}(\alpha_{10} + J_2) s^2 - \frac{1}{3}(\gamma_1 + \alpha_{11} + J_3 - \frac{1}{2} J_1^2) s^3 -$$

$$- \frac{1}{4}[\alpha_{30} + \alpha_{12} + J_4 - \frac{2}{3} J_1(\alpha_{10} + J_2)] s^4 -$$

$$- \frac{1}{5}[\gamma_2 + \alpha_{31} + \alpha_{13} + J_5 - \frac{7}{12} J_1(\gamma_1 + \alpha_{11} + J_3) -$$

$$- \frac{1}{6}(\alpha_{10} + J_2)^2 + \frac{1}{24} J_1^3] s^5 + \ldots$$

$$M_{12} = s - \frac{1}{6} J_1 s^3 - \frac{1}{12}(\alpha_{10} + J_2) s^4 - \frac{1}{20}(\gamma_1 + \alpha_{11} + J_3 - \frac{1}{6} J_1^2) s^5$$

$$- \frac{1}{30}[\alpha_{30} + \alpha_{12} + J_4 - \frac{1}{4} J_1(\alpha_{10} + J_2)] s^6 + \ldots$$

$$M_{22} = 1 - \frac{1}{2} J_1 s^2 - \frac{1}{3}(\alpha_{10} + J_2) s^3 -$$

$$- \frac{1}{4}(\gamma_1 + \alpha_{11} + J_3 - \frac{1}{6} J_1^2) s^4 -$$

$$- \frac{1}{5}[\alpha_{30} + \alpha_{12} + J_4 - \frac{1}{4} J_1(\alpha_{10} + J_2)] s^5$$

$$(40)$$

(These truncated power series give at least four significant figures accurately, which is enough for our purpose).

This, of course, is the matrix which transforms from 0 to s. For the first part of the fringe field we use the inverse matrix to transform from -s to 0 (not the time-reversed matrix, since we do not want to reverse the sign of the velocity).

For the z-oscillations we need only set every $\gamma_i = 0$

and reverse the sign of every α_{mn} and J_m to satisfy (30)
instead of (29).　In those parts of the magnet where　$F(s)= 1$,
we can use the smae expansion of $\frac{R_1}{R(s)} \sec \phi(s)$ to find the
correction terms due to the variation of n.　The effect is
of course much smaller, since n rises quadratically from its
value at the center of a magnet and the ends,　which give the
major contribution to the effect in hard edge approximation
have now been eaten away by the fringe field.　When we
expand about the center of a magnet　$\phi(0) = 0$ and therefore
$A_1 = 0$.　(29)　and (30) then reduce respectively, where
$F(s) = +1$, to

$$x'' + \left[\frac{1+n_1}{\rho_0^2} + \frac{A_2 n_1}{\rho_0^2} s^2 + \cdots \right] x = 0 \tag{41}$$

$$3'' - \left[\frac{n_1}{\rho_0^2} + \frac{A_2 n_1}{\rho_0^2} \right] 3 = 0 \tag{42}$$

Since the effect is so small, we keep only the first
correction term.　For (41)

$$
\begin{cases}
M_{11} = \cos \frac{\sqrt{1+n_1}}{\rho_0} s - \frac{1}{12} \frac{n_1 A_2}{\rho_0^2} s^4 \\[2mm]
M_{21} = - \frac{\sqrt{1+n_1}}{\rho_0} \sin \frac{\sqrt{1+n_1}}{\rho_0} s - \frac{1}{3} \frac{n_1 A_2}{\rho_0^2} s^3 \\[2mm]
M_{12} = \frac{\rho_0}{\sqrt{1+n_1}} \sin \frac{\sqrt{1+n_1}}{\rho_0} s - \frac{n_1 A_2}{\rho_0^2} s^5 \\[2mm]
M_{22} = \cos \frac{\sqrt{1+n_1}}{\rho_0} s - \frac{1}{4} \frac{n_1 A_2}{\rho_0^2} s^4
\end{cases}
\tag{43}
$$

and for (42)

$$
\begin{cases}
M_{11} = \cosh \dfrac{\sqrt{n_1}}{\rho_0} s + \dfrac{1}{12} \dfrac{n_1 a_2}{\rho_0^2} s^4 \\[2mm]
M_{21} = \dfrac{\sqrt{n_1}}{\rho_0} \sinh \dfrac{\sqrt{n_1}}{\rho_0} s + \dfrac{1}{3} \dfrac{n_1 a_2}{\rho_0^2} s^3 \\[2mm]
M_{12} = \dfrac{\rho_0}{\sqrt{n_1}} \sinh \dfrac{\sqrt{n_1}}{\rho_0} s + \dfrac{1}{20} \dfrac{n_1 a_2}{\rho_0^2} s^5 \\[2mm]
M_{22} = \cosh \dfrac{\sqrt{n_1}}{\rho_0} s + \dfrac{1}{4} \dfrac{n_1 a_2}{\rho_0^2} s^4
\end{cases}
\tag{44}
$$

Where $F(s) = -1$, the matrix elements have analogous form, but the orbit length in the magnet is so short that the effect is quite negligible.

The product of these matrices in the appropriate order is then the transformation matrix from the center of a radially focussing magnet to the center of a radially defocussing magnet.

σ may be calculated in the same way as it was above for hard-edge orbits.

Such calculations have been done for the soft-edge orbits given above in Section V and for some others. In order that hasty conclusions will not be drawn, we will defer presentation of these results to a later report, where more comprehensive results will be given.

Amplitudes of oscillation may also be calculated from the

transformation natrix. These also will be discussed in later report.

Note: The cancellation discussed above which makes δ small does not occur for F(s) such that $\frac{dF}{ds}(b)$ is small. This may make it necessary to recalculate β_1' using the value of δ from the first approximation.

DETAILED CALCULATIONS OF A SMALL
MODEL FFAG MARK Ib ACCELERATOR*
PART B

F. T. Cole[+]

Midwestern Universities Research Association

This report is a continuation of a report of the same title
(MURA-FTC/DWK-1) by D. W. Kerst and the present writer, which will be re-
ferred to as A. In A methods were developed for discussing orbits in a
Mark Ib FFAG model in which the vertical focussing depends strongly on
"edge" focussing. The present report will amplify some points of A and
give results of calculations done to date.

I. FURTHER DISCUSSION OF THE METHODS OF A.

1.   Equation (19) of A can be derived also from the Lorentz force equation using the R equation (A.20) and the relation between θ and s, both of which are geometrical relations following from inspection of the figure on page 19 of A. In cylindrical coordinates

$$\frac{d}{dt}\left(m \frac{dR}{dt} \right) = m R \dot{\theta}^2 - \frac{e}{c} R \dot{\theta} H_3 \tag{1}$$

where m is the total mass. For a particle of constant speed

$$\ddot{R} = R \dot{\theta}^2 - \frac{e}{c} \frac{R \dot{\theta} H_3}{m} \tag{2}$$

We introduce the new independent variable s (arc-length) by

$$\frac{ds}{dt} = v = \text{constant.} \tag{3}$$

Then

$$\frac{d}{ds}\left(\frac{dR}{ds} \right) = R \frac{\dot{\theta}^2}{v^2} - \frac{e}{c} \frac{R \dot{\theta} H_3}{m v^2} \tag{4}$$

$$\frac{\dot{\theta}}{v} = \frac{d\theta}{dt} \frac{dt}{ds} = \frac{d\theta}{ds} = \frac{\cos \phi(s)}{R(s)} \tag{5}$$

from the figure on page 19 of A.

From (A.20),

$$\frac{dR}{ds} = - \sin \phi(s) \qquad \text{, so that}$$

$$- \frac{d}{ds}(\sin \phi) = - \cos \phi \frac{d\phi}{ds} = \frac{\cos^2 \phi}{R} - \cos \phi \frac{e}{c} \frac{H}{m v}$$

and since

$$p = m v = \frac{e}{c} \rho H_3 = \frac{e}{c} \rho_0 H_0 \tag{6}$$

and

$$H(x,s) = H_o(x) F(s),$$

(7)

$$\frac{d\phi}{ds} = \frac{1}{\rho_o} F(s) - \frac{\cos\phi}{R}$$

(8)

which is (A.19).

2.   The ambiguity involved in the ϕ and R equations ((19) and (20) of A) which is discussed on page 19 of A may be eliminated by considering a function F defined in space rather than along the orbit. Such a function does not depend on the position of the orbit. Suppose that, in the two dimensional space of the median plane we use the position variables R and Θ. The magnetic field

$$H(R,\Theta) = H_o F(R,\Theta)$$

(9)

and

$$p = \frac{e}{c} \rho_o H_o$$

(10)

As in A, the turning due to the magnetic field is in distance ds

$$d\varphi = \frac{dp}{p} = \frac{\frac{e}{c} H_o F(R,\Theta) ds}{\frac{e}{c} \rho_o H_o}$$

and from this must be subtracted the change of ϕ due to the change of Θ. The closed orbit equations may then be written

$$\begin{cases} \dfrac{d\phi}{d\Theta} = \dfrac{R}{\rho_o} F(R,\Theta) \sec\phi - 1 \\ \dfrac{dR}{d\Theta} = - R \tan\phi \end{cases}$$

(11)

These equations are more difficult to solve for the closed orbit than the

ϕ and R equations of A, and since we saw in A that the orbit depends strongly only on $\int F(s)ds$, Θ_1' and Θ_2', it does not seem worthwhile to do more than point out the possibility of resolution of the ambiguity.

3.   In Sec. III of A, the transformation matrix for hard edges is derived using an infinite force at the edge of a magnet. At first sight this appears strange, since all the forces in a real magnetic field are finite and the focussing effects of edges are physically due to different path lengths in the magnetic field. The δ - function which gives rise to this infinite force arises from the linear approximation because one takes the derivative $\frac{dH}{dx}$ and $F(s)$ is essentially a step-function in x because of the different path length.

The result can be derived without reference to infinite forces. To first order in x, the difference in path length between the equilibrium orbit and an orbit of displacement x is

$$\delta s = x \tan \phi \qquad (12)$$

as on page 12 of A.

The angle turned through due to the magnetic field in this distance is

$$\frac{d\phi}{p} = \frac{\frac{e}{c} H \frac{ds}{dt} dt}{\frac{e}{c} \rho H} = \frac{\delta s}{\rho} + O(x) \qquad (13)$$

and there is thus (to first order in x) a change in angle $\left(\frac{dx}{ds} \right)$ for a particle of displacement x by an amount

$$\Delta \left(\frac{dx}{ds} \right) = \frac{\delta s}{\rho} = \frac{x \tan \phi}{\rho} \qquad (14)$$

from which the transformation matrix for edges (A.13) follows immediately. This is essentially the same derivation as that of Jones (MURA-LWJ-7).

4.   The estimate of the correction term δ on page 22 of A depends on the

approximation

$$F'(s) \cong -\frac{2}{s^3}$$

which is valid only when the fringe field is close to a linear function of distance. When a fringe field of the form

$$F(s) = a_1 s + a_3 s^3 \tag{15}$$

with the same net turning $\left(\int F(s) ds\right)$ from b to the point where $F''(s) = c$ and from this point to c is used, the series given in A for δ converges very slowly. If the series is truncated after the terms given on page 22 of A, one finds a value for δ of -1.7. This gives an R_c and an R_2 smaller than the values for the linear fall-off law

$$F(s) = a_1^L s, \tag{16}$$

whereas they should be greater, since the "cubic" fall-off law (15) begins to fall off sooner than the linear law (16), and the orbit therefore moves out.

We must therefore estimate the value of δ in a different way. We denote quantities pertaining to a linear fall-off by a superscript L and quantities referring to a cubic fall-off law by a superscript C. Then

$$\begin{cases} R_c^C = R_b^C + \int_0^{s'} \sin \phi^C \, ds \\ R_c^L = R_b^L - \int_0^{s'} \sin \phi^L \, ds \end{cases} \tag{17}$$

where R_b^L and R_c^L are evaluated at b and C for the cubic law, so that s is the same variable for both fall-off laws. From (17),

$$\left| (R_c^c - R_c^L) - (R_b^c - R_b^L) \right| = \left| \int_0^{S^1} (\sin\phi^L - \sin\phi^c)\, ds \right|$$

$$= 2 \left| \int_0^{S^1} \sin\tfrac{1}{2}(\phi^L - \phi^c) \cos\tfrac{1}{2}(\phi^L + \phi^c)\, ds \right|$$

$$< a \left| \int_0^{S} \sin\tfrac{1}{2}(\phi^L - \phi^c)\, ds \right| < \left| \int_0^{S} (\phi^L - \phi^c)\, ds \right| \tag{18}$$

Now

$$\left| \int_0^{S} (\phi^L - \phi^c)\, ds \right| = \left| \int_0^{S^1} \int_0^{S} \left(\frac{d\phi^L}{ds'} - \frac{d\phi^c}{ds'} \right) ds'\, ds \right|$$

$$= \left| \int_0^{S^1} \int_0^{S} \left\{ \frac{F^L(s') - F^c(s')}{\rho_o} - \frac{d}{ds'}(\theta^L - \theta^c) \right\} ds'\, ds \right|$$

$$< \left| \frac{1}{\rho_o} \int_0^{S^1} \int_0^{S} (F^L(s') - F^c(s'))\, ds'\, ds \right| + \left| \int_0^{S^1} (\theta^L - \theta^c)\, ds \right| \tag{19}$$

The two fall-off lens should have $F(s) = 0$ at the same θ, since this is determined separately (see Sec. 1 of A); thus $\theta^L = \theta^c$ where $F(s) = 0$ and at b and c. θ changes by about $18°$ from b to c, so it seems safe to assume

$$|\theta^L - \theta^c| < 1° \simeq 0.02$$

Then

$$\left| \int_0^{S} (\theta^L - \theta^c)\, ds \right| < 0.02\, S' \sim 0.2 \tag{20}$$

The integrals of the first absolute value sign of (19) can be performed using (15) and (16). The coefficients a_i are determined by

$$\begin{cases} F^L(-S_1^L) = +1 \\ F^c(-S_1^c) = +1 \\ F^L(+S_2^L) = -1 \\ F^c(+S_2^c) = -1 \end{cases} \tag{21}$$

for the left and right halves of the "straight section" using Vogt-Wilsen's curves. In the cubic case, the other coefficients are fixed by the requirement that

$$\begin{cases} \int_b^o F^L ds = \int_b^o F^c ds \\ \int_0^c F^L ds = \int_0^c F^c ds \end{cases} \tag{22}$$

where o is the point where $F(s) = 0$. This gives the same net turning in the cubic and linear cases.

The result of the evaluation of the first integral of (19) is a lengthy sum of simple functions of S_i^L, S_i^c and the differences $\left(S_i^c - S_i^L\right)$ and $\left(S_2^c - S_2^L\right)$. The result is small for values of S_i^L and S_i^c in the range of interest. If we take

$$\begin{cases} S_1^L = S_2^L = 5 \text{ cm.} \\ S_1^c = S_2^c = 6 \text{ cm} \\ \rho = 80 \text{ cm.} \end{cases}$$

the whole term has a value 0.03. If we take

$$\begin{cases} S_1^L = S_2^L = 5 \text{ cm.} \\ S_1^c = S_2^c = 7 \text{ cm.} \\ \rho = 20 \text{ cm.} \end{cases}$$

we find a value 0.04. The exact value is not important, since the ● term appears to be larger.

Thus it is safe to estimate

$$\left| (R_c^c - R_c^L) - (R_b^c - R_b^L) \right| < 0.3 \text{ cm.} \tag{23}$$

δ is quite small ($\sim 0.1\, cm$) for the linear fall-off law and the difference

$$R_b^c - \wedge_b^L \qquad \text{as calculated by the closed orbit method of A is small.}$$

Therefore δ for the cubic fall-off law must also be quite small and may be neglected.

Experience with the closed orbit calculation shows that the value of α affects the numerical results much less than that of δ .

5.   There is an error in equation (32) of A.   The term

$$\frac{\sin \phi_0}{R_0}$$

in $\wedge_1$, and the terms

$$\frac{\sin^2 \phi_0}{R_0} + \frac{\cos \phi_0}{2 R_0} \phi_0'$$

in $\wedge_2$ should be multiplied by

$$\wedge_0 = \sec \phi_0$$

These terms always appear in the series combined with other (γ_i and δ_i) terms which are much larger, so that the error affects only the fourth significant figure of the frequencies obtained.   The error also enters in equations (43) and (44), but there $\wedge_t = 1$ and the error vanishes.

The error in equation (32) was pointed out by Mr. G. Mohan.

II. SOFT EDGE RESULTS.

The frequencies of oscillation about equilibrium orbits for various soft edges have been calculated by the methods described in A.   The cases were chosen with the two purposes in mind of choosing the magnet geometry for the Mark Ib model and of exploring the importance of various physical effects.   Because of the greater emphasis on the first of these objectives, no general survey of the working diagram has been made, but some comments can be made about the physics of soft edges.

In the tables below we give the following parameters: 1) Gap - the vertical distance between iron pole surface, which determines the distance into the magnets to which the soft edges extend; 2) ϵ_1 and ϵ_2 - the angles of the magnet edges measured from the center of the machine, which determine the geometry of the median plane; 3) n_1 - the value of n at the center of the wide (radially focussing) magnet; 4) Zero shift - the distance along the orbit that the point where $F(s) = C$ is shifted toward the wide pole because of different field strengths at the same radius in the two magnets; 5) ϕ_0 - the value of ϕ at the point where $F(s) = 0$; and 6) $\bar{\nu}_x$ and $\bar{\nu}_3$ - the number of radial and vertical oscillations per revolution.

We show first the effect of different "eat-in" distances due to different gap sizes.   We give results for the hard-edge case, for a gap of 4 cm, for a gap of 5.644 cm, which is the gap at the high energy radius obtained by scaling up photographically from a gap of 4 cm at the injection radius and for a gap of 6.5 cm, obtained by scaling up from 4 cm at the inner radius of the vacuum tube.   In these calculations the fall-off law was taken as a linear function of distance.   In addition, the variation of n within the magnets (but not in the fringe fields) was omitted.

	Gap	η_1	ϵ_1	ϵ_2	Zero Shift	ϕ	ν_x	ν_3
	Hard Edge	1.51	13.17°	4.93°	-----	-------	2.87	1.74
1.	4.0	1.51	13.17	4.93	0.13	0.3532	2.94	1.65
2.	5.644	1.51	13.17	4.93	0.13	0.3403	2.98	1.48
3.	6.5	1.51	13.17	4.93	0.13	0.3318	2.97	1.37

The effect of the η- variation within the magnets is smaller than in the hard-edge case calculated in A, because it extends over a smaller length of orbit. We give two examples.

	Gap	γ_1	θ_1	ϵ_1	Zero Shift	ϕ	ν_μ	ν_j	η-variation
2.	5.644	1.51	13.17°	4.93°	0.13	0.3403	2.98	1.48	No
4.	5.644	1.51	13.17	4.93	0.13	0.3403	3.04	1.45	Yes
1.	4.0	1.51	13.17	4.93	0.13	0.3532	2.94	1.65	No
5.	4.0	1.51	13.17	4.93	0.13	0.3532	3.01	1.61	Yes

The effect of the zero shift is shown in the following example.

	Gap	η_1	ϵ_1	θ_2	Zero Shift	ϕ	ν_μ	ν_j
6.	5.644	1.51	13.17°	4.93°	0	0.3328	2.92	1.41
2.	5.644	1.51	13.17	4.93	0.13	0.3403	2.98	1.48

Varying n and the geometry produce the same qualitative effects as in the hard-edge approximation, as shown in the examples below, which all use linear fall-off laws.

	Gap	ν_1	θ_1	θ_2	Zero Shift	ϕ_c	ν_R	ν_z
2.	5.644	1.51	13.17°	4.93°	0.13	0.3403	2.98	1.48
7.	5.644	1.40	12.61	5.03	0.13	0.3727	3.16	1.89
8.	6.5	1.3	12.87	5.22	0.13	0.3627	2.96	1.79
9.	6.5	1.2	12.87	5.22	0.13	0.3627	2.80	1.81

The effect of the shape of $F(s)$ is shown in the following example. The first calculation uses a linear fall-off law, as in equation (16) of this report, while the second uses a cubic law as in equation (15), with the same net turning $\left(\int F(s)ds \right)$ to the point where $F(s) = 0$ as the linear law.

	Gap	n_1	θ_1	θ_2	Zero Shift	ϕ	ν_x	ν_z	Fall-off Law
9.	6.5	1.2	12.87	5.22	0.13	0.3627	2.80	1.81	Linear
10.	6.5	1.2	12.87	5.22	0.13	0.3655	2.81	1.71	Cubic

While it is difficult to draw general conclusions from numerical examples, the results seem to be susceptible to some physical interpretation. As the edges "soften," ν_x increases slightly and ν_z decreases much more. The two main causes appear to be: first, the negative pole is "eaten into" proportionally more than the positive pole, so that there is more radial and less vertical focussing; second, the angle ϕ, which has a defocussing effect on the radial and a focussing effect on the vertical motion, is smaller all along the orbit in softer edges. This follows from the equation of motion (in integrated form.)

$$\Delta\phi = \frac{1}{p_c} \int_{s_c}^{s_1} F(s)ds - \Delta\theta$$

Even when the net turning due to the magnetic field $\left(\int F(s)ds \right)$ is the same for each side of the "straight section" in soft as in hard edges, the integral

reaches its full value at a larger   in soft edges, so that the negative $\Delta \epsilon$ term is larger and $\ \ /$ is smaller.

Comparison of 8 and 9 shows that ν_j is almost independent of η, while 1, 2 and 3 show that ν_x is almost independent of ϕ, just as in the hard edge approximation. It appears from this that the smooth approximation rule

$$\sigma_{total} = \sqrt{\sigma_{edge}^2 + \sigma_{interior}^2}$$

is qualitatively correct.

The vertical frequency ν_j appears to be almost directly proportional to ϕ, the value of ϕ at the point where $F'(z) = 0$, which is close to the maximum value of ϕ. This is true except for case 10, which has a smaller than case 9. This may be explained by noting that the cubic fall-off law eats further into the magnets than the linear law, so that ϕ has smaller values for a large fraction of the orbit. $\frac{f'}{f}$ is also smaller for a large fraction of the orbit in the cubic case. (A useful check on the computations at any stage is the determinant of the transformation matrix, which should be unity. Calculation of this determinant aids materially in quickly finding errors. It must be noted that by this criterion the cubic calculation (case 10) is less accurate ($\sim 1/4$) than the linear (case 9) (~ 0.2). A previous cubic calculation with about 2% error gave $\nu_\phi = 1.70$, so that the present result might be a slight underestimate. However, it appears almost certain that the cubic is smaller than the linear.)

At first sight, comparison of 2 and 7 seems to give a strange result. When the positive (radially focussing) pole is shortened, ν_x increases rather than decreases. This paradoxical result may be resolved by consulting the closed orbit data given in A on page 24, where the first line is our case 2 and the fifth line is our case 7. In our case 7 the whole orbit has moved out to larger radii and therefore ρ' is larger, giving greater radial focussing.

The main effect of the zero shift is to move the equilibrium orbit into smaller radii (the equilibrium orbit for this case is given by the third line of the table on page 24 of A,) so that β_1' and ϕ are smaller. Therefore both ν_R and ν_z decrease.

The largest physical effect of softening the edges appears to be the change in the values of ϕ along the orbit. The effect on the relative magnetic lengths of the magnets seems to be somewhat smaller, since ν_R does not change by too much as the edges soften. However, the hard edge approximation gives poor results for the radial motion also, because of the movement of the equilibrium orbit.